ELSEVIER

Thin Solid Films 273 (1996) 304–307

thin solid films

Scanning force microscopy application to polymer surfaces for novel nanoscale surface characterization

Makoto Motomatsu [a], Heng-Yong Nie [b], Wataru Mizutani [b], Hiroshi Tokumoto [b]

[a] *Joint Research Center for Atom Technology (JRCAT), Angstrom Technology Partnership (ATP), Higashi 1-1-4, Tsukuba, Ibaraki 305, Japan*

[b] *Joint Research Center for Atom Technology (JRCAT), National Institute for Advanced Interdisciplinary Research (NAIR), Higashi 1-1-4, Tsukuba, Ibaraki 305, Japan*

Abstract

The techniques of scanning force microscopy have been successfully used to investigate phase-separated polymer surfaces on a nanometer scale and been proved to be of great advantage in surface characterization studies of polymers. We observed two kinds of phase-separated surfaces of polystyrene (PS)–polyethylene oxide (PEO) blend film and injection molded crystalline engineering polymer (acetal resin)–elastomer blend plate. In the local mechanical property measurement of the PS–PEO samples, PEO domains were found to be softer and show higher friction force than PS domains with the lateral resolution of less than 100 nm. The results agree qualitatively with those of the bulk. In the local friction measurement of the acetal resin–elastomer blend plate, the surface showed stripe structures 100–300 nm wide: the lower friction region corresponds to acetal resin and the higher one to elastomer. However, in the local elasticity measurement, the difference between the two could not be detected presumably due to the subsurface effect.

Keywords: Polymers; Surface structure; Atomic force microscopy

1. Introduction

Recently, it has become increasingly important to observe or characterize organic materials on solid substrates with a high spatial resolution and without any special surface treatment in air. Scanning force microscopy (SFM) [1,2] enables us to observe surface topography on a nanometer scale together with local mechanical properties such as friction force and stiffness [3–9], in contrast to the conventional methods such as static time of flight–secondary ion mass spectroscopy (TOF–SIMS) or Auger electron spectroscopy (AES) whose resolution is limited by the beam size. We thus employ the SFM technique to investigate polymer surfaces and identify individual polymers by measuring their own mechanical properties. However, the relation between the microscopic and macroscopic mechanical properties is still unknown. In order to solve this problem, we have studied the surface properties of phase-separated polymers and compared them with the bulk ones [6,8].

In this paper we shall present the experimental results on a polystyrene (PS)–polyethylene oxide (PEO) polymer blend film as a model system and on injection molded crystalline engineering polymer (acetal resin)–elastomer blend plate.

2. Experimental

PS and PEO were blended in benzene at 1:1 wt. ratio with the concentration of 2 wt.%. The solution was spin-coated onto a freshly cleaved mica substrate at 2 000 rpm, then annealed under vacuum (0.5 Torr) at 90 °C for 24 h to remove residual solvent. The film thickness thus obtained was 200–300 nm. The characteristics of the individual polymers used are summarized in Table 1. The crystalline acetal resin–elastomer blend materials were injected from the melt to a dumbbell test piece molder of 3 mm thickness.

SFM measurements were carried out using a commercial atomic force microscope (SPA-300, Seiko Instruments Inc., Japan) in the contact mode at 1×10^{-9} N in air. A V-shaped

Table 1
The characteristics of PS and PEO

	PS	PEO
M_w	19 600	100 000
d	1.05	1.13
T_g	110 °C	-67 °C
T_m	-	66 °C

M_w, weight-average molecular weight; d, density; T_g, glass transition temperature; T_m, melting temperature.

SSDI 0040-6090(95)06792-2

microfabricated cantilever (Olympus Opt. Inc.) with a length of 100 μm, Si_3N_4 pyramidal tip, and a spring constant of 0.1 N m^{-1}, was used. The local friction was measured using a four-segment photodiode system and its absolute value was estimated from the dimension, the material of the cantilever and the sensitivity of the detection system using the formula proposed by Meyer and Amer [10]. The local stiffness was measured by modulating the sample along the z direction. The modulation amplitude was set at about 1 nm and the frequency at 5 kHz. The cantilever defection caused by the sample modulation along the z direction was measured with the lock-in technique [2,11].

3. Results and discussion

We have already shown that PS and PEO are incompatible, leading to phase-separated structures [8]. In addition, these two polymers are found to be easily distinguished by their different natures and mechanical behavior, amorphous and hard for PS while crystalline and soft for PEO [12,13]. Fig. 1(a) is an atomic force microscopy (AFM) image showing typical phase-separated domains with an amorphous region which corresponds to PS and clear lamella regions indicated by the arrows in Fig. 1(a) which is a typical structure of PEO crystal. The domain size was distributed from 100 nm to several microns depending on the position. Fig. 1(b) shows a schematic drawing of the structure which consists of the amorphous PS and the underlying crystallized PEO on the mica substrate. Guzonas et al. proposed that there exists a specific interaction (ion–dipole interaction) of PEO with mica substrates, resulting in the strong adhesion of PEO to mica surfaces [14]. The annealing temperature of 90 °C was set between the melting temperature of PEO and the glass transition temperature of PS (Table 1) and the annealing time of 24 h could be long enough for PEO to crystallize and for PS to segregate to the surface. Säkellariou also confirmed significant surface enrichment of PS in PS–PEO blend system by surface-energy measurements [13].

On both domains, we carried out friction force measurements. Since the torsion signal of the AFM cantilever was enhanced by the tip jump-up effect caused by the height difference between PS and PEO as well as typical steps of PEO lamella structure, we could not obtain a clear friction force map. However, by the friction force loop measurement (Fig. 1(c)) along the forward and backward scans on each domain (indicated by black lines in Fig. 1(a)), we confirmed that PEO showed higher friction force by ca. 3 nN than PS (estimation value [10]). It should be mentioned that the apparent friction depends on the contact area between the tip and surface. In the present case, the higher friction force of PEO would originate from the increase of the contact area due to the softness. In addition, in the local elasticity measurement on each domain, we could detect the stiffness difference with a lateral resolution of less than 100 nm [14]. Fig. 2(a) and 2(b) show an AFM topography image showing

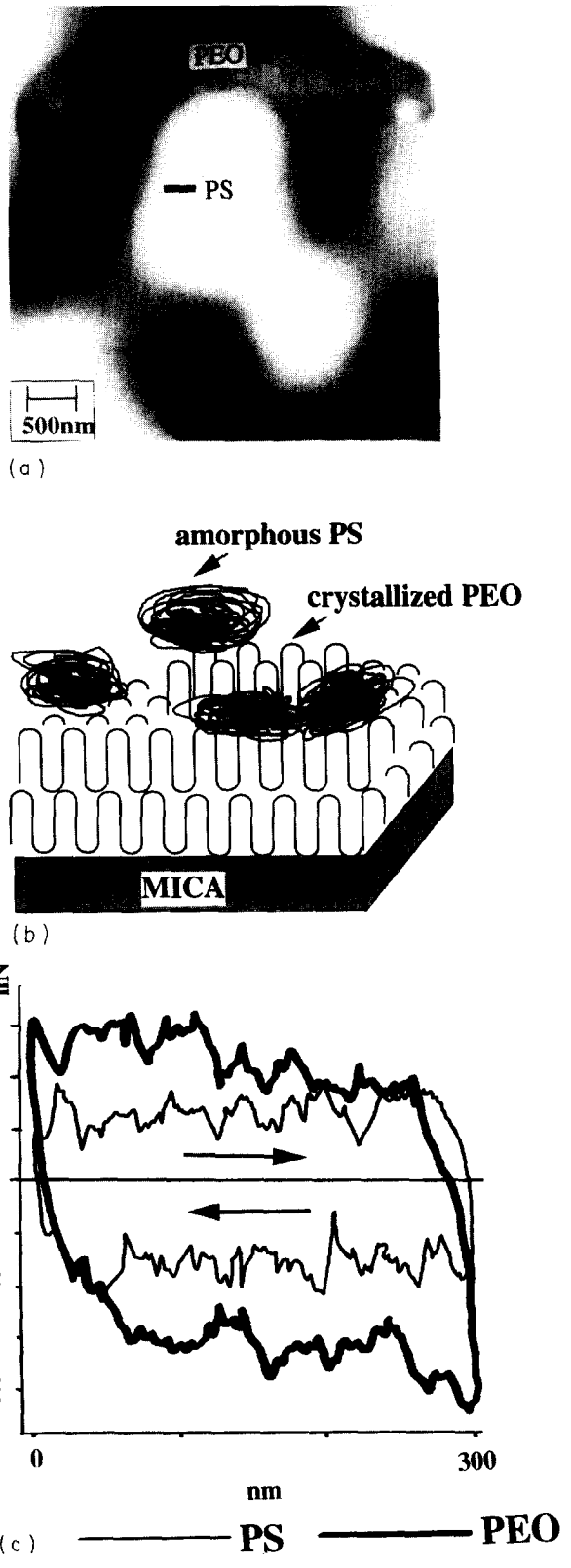

Fig. 1. AFM image (a), schematic drawing (b), and friction force loop (c), (scan length, 300 nm; PS, plain line; PEO, bold line) of phase-separated PS–PEO blend film surface. In (a), the gray scale for the height is 110 nm and the typical lamella structures of PEO were indicated by the arrows. In (c), the tip was scanned from the left to the right and from the right to the left on the scanning positions indicated by black lines in (a).

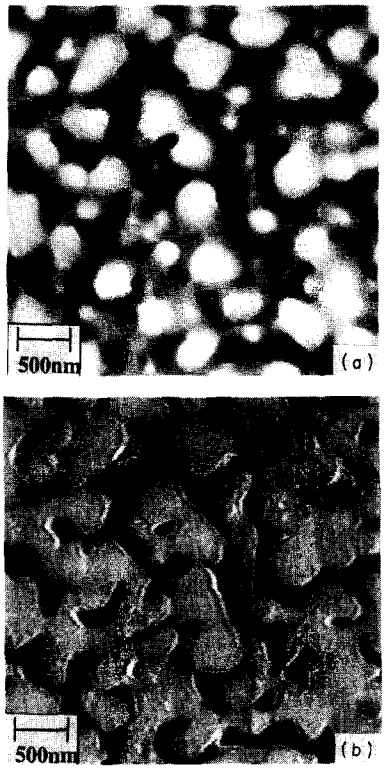

Fig. 2. AFM topography (a) and stiffness (b) images of the same area of PS–PEO blend film showing worm-like domains of 100 nm to a few microns in size. The gray scale for the height in (a) is 60 nm. In (b), bright region corresponds to higher stiffness (PS) and dark region to lower stiffness (PEO).

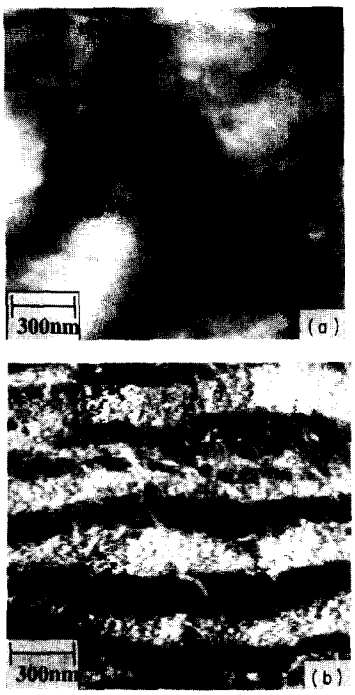

Fig. 3. AFM (a) and friction (b) images of injection molded crystalline acetal resin–elastomer blend plate. In (a), the gray scale for the height is 45 nm. In (b), the bright region corresponds to higher friction (elastomer) and the dark region to lower friction (acetal resin).

worm-like domains and the stiffness map of the same area indicating clear mapping of PEO and PS domains on the surface, respectively. This stiffness map clearly shows that PEO regions are softer (dark regions) than PS regions (light regions). These mechanical properties agree with those of the bulk qualitatively.

We also applied these techniques to the injection-molded crystalline acetal resin–elastomer blend surfaces. Fig. 3(a) and 3(b) show the AFM topography and the friction force images of the same area, respectively. The topography with a height difference of 20–30 nm reflects the surface roughness of the opposite molder material. In contrast, in the friction image, stripes with 100–300 nm wide reflect the injected resin flow direction. We did not observe such structures on the injection molded acetal resin homopolymer. The estimated friction force difference was ca. 1.7 nN [10]. We attribute the lower friction regions (dark area) to the acetal resin and the high friction regions (bright area) to the elastomer based on the macroscopic friction force coefficients test data. On the other hand, we could not detect the significant difference between the two regions by the local stiffness measurement. This is somewhat surprising since, according to the Young's modulus of the bulk, the acetal resin is 10–100 times harder than the elastomer. This mystery could be explained by the subsurface effect as well as the sensitivity of the instrument. The force modulation data of soft materials should be influenced by subsurfaces, in other words, the thickness of the material on the topmost surface. Fig. 4 shows a schematic drawing of the cantilever response influenced by the thickness of the soft elastomer. The tip-induced pressure deforms the material and distributes along the z axis. Then the measured stiffness of the elastomer would be influenced substantially by the subsurface acetal resin layer, when the penetration of the AFM tip is much larger than the thickness of the elastomer.

We shall estimate the effect of the acetal resin to the stiffness of the elastomer in the present case. From Hertz theory

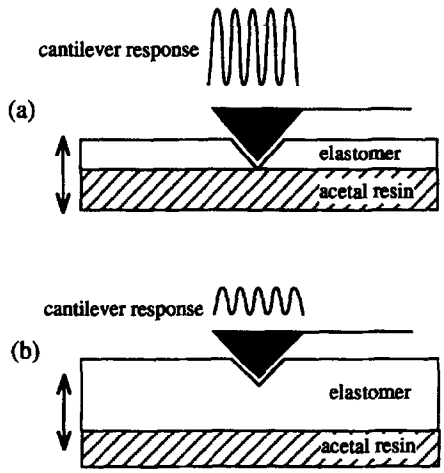

Fig. 4. Schematic drawing of cantilever response as a result of the deformation of the soft elastomer layers (thin (a) and thick (b) compared with the oscillation amplitude of the sample shown by arrows) on the subsurface hard acetal resin.

of elastic contact [15], the contact radius (r) is found to be $r \propto E^{-1/3}$ (E is the elasticity of the object) by assuming that the AFM tip material is much harder and the Poisson's ratio of the acetal resin is the same with that of the elastomer. When we apply the bulk result that the acetal resin is 10–100 times harder than the elastomer, the contact radius of the soft elastomer is about 2.2–4.6 times larger than that of the hard acetal resin due to the deformation of the AFM tip. This means that the penetration depth of the AFM tip is larger than the elastomer thickness and the measured local stiffness would be influenced by the acetal resin as shown in Fig. 4(a). Thus, it would be difficult to distinguish the elastomer from the acetal resin from the local stiffness measurement. On the other hand, in the friction force microscopy, the larger contact area of the soft elastomer enhances signals so that it becomes useful.

4. Conclusion

We demonstrated here the high potential of the SFM as a novel surface analysis tool with visible mapping of the different mechanical properties, using a model system of phase-separated PS–PEO blend film and a practical system of the injection molded crystalline acetal resin–elastomer blend surface. The lateral resolution was 100 nm which was not realized so far by other surface analysis methods. In the PS–PEO blend system, PEO domains showed larger friction force by ca. 3 nN and lower stiffness than PS domains with the SFM technique. We confirmed these local results agreed with those of the bulk qualitatively, although it is not easy to discuss the absolute values quantitatively because of experimental uncertainty. In the acetal resin–elastomer blend system, the elastomer region showed larger friction force than the acetal resin region. Such a nanoscale phase-separated structure (stripes with 100–300 nm in width) on surfaces which was caused by their immiscibility has never been observed. In contrast, in the local elasticity measurement, the difference could not be detected. The obtained stiffness results here will presumably include the information that the topmost surface of the elastomer is deformed by the AFM tip and the cantilever response is influenced by the subsurface hard acetal resin.

Acknowledgements

We acknowledge Mr. Tatsuhiro Takahashi and Mr. Hiroshi Tashiro of Du Pont Kabushiki Kaisha for helpful discussions and supplying the injection molded crystalline acetal resin–elastomer samples. This work was supported by the New Energy and Industrial Technology Development Organization (NEDO).

References

[1] C.M. Mate, G.M. McClelland, R. Erlandsson and S. Chiang, *Phys. Rev. Lett., 59* (1987) 1942.
[2] P. Maivald, H.J. Butt, S.A.C. Gould, C.B. Prater, B. Drake, J.A. Gurley, V.B. Elings and P.K. Hansma, *Nanotechnology, 2* (1991) 103.
[3] E. Meyer, R.M. Overney, R. Lüthi, D. Brodbeck, L. Howald, J. Frommer, H.-J. Güntherodt, O. Wolter, M. Fujihira, H. Takano and Y. Gotoh, *Thin Solid Films, 220* (1992) 132.
[4] T. Kajiyama, K. Tanaka, I. Ohki, S-R. Ge, J-S. Yoon and A. Takahashi, *Macromolecules, 27* (1994) 7932.
[5] R.M. Overny, E. Meyer, J. Frommer, H.-J. Güntherodt, M. Fujihira, H. Takano and Y. Gotoh, *Langmuir, 10* (1994) 1281.
[6] M. Motomatsu, H.-Y. Nie, W. Mizutani and H. Tokumoto, *Jpn. J. Appl. Phys., 33* (1994) 3775.
[7] T. Yuba, S. Yokoyama, M. Kamimoto and Y. Imai, *Adv. Mater., 6* (1994) 888.
[8] M. Motomatsu, W. Mizutani, H.-Y. Nie and H. Tokumoto, *Book Forces in Scanning Probe Methods*, Güntherodt et al. (Eds), Kluwer, Netherlands, 331 pp.
[9] S.O. Akari, E.W. van der Vegte, P.C.M. Grim, G.F. Belder, V. Koutsos, G. ten Brinke and G. Hadziioannou, *Appl. Phys. Lett., 65* (1994) 1915.
[10] G. Meyer and N. Amer, *Appl. Phys. Lett., 57* (1990) 2089.
[11] H.-Y. Nie, M. Motomatsu, W. Mizutani and H. Tokumoto, *J. Vac. Sci. Technol., B13 (8)* (1995) 1163.
[12] S. Tsitsilianis, G. Staikos, A. Dondos, P. Lutz and P. Rempp, *Polymer, 33* (1992) 3369.
[13] P. Säkellariou, *Polymer., 34* (1994) 3408.
[14] D.A. Guzonas, D. Boils, C.P. Tripp and M.L. Hair, *Macromolecules, 25* (1992) 2434.
[15] K.L. Johnson, *Contact Mechanics*, Cambridge University Press, Cambridge, 1985.